## PRIMARY RESEARCH PAPER



# Diatom-Diazotroph Associations in hydrographically defined habitats of the South China Sea

Lam Nguyen-Ngoc · Sarah C. Weber · Hai Doan-Nhu · Ajit Subramaniam · Maren Voss · Joseph P. Montoya

Received: 16 January 2023 / Revised: 6 June 2023 / Accepted: 10 June 2023 / Published online: 22 June 2023 © The Author(s), under exclusive licence to Springer Nature Switzerland AG 2023

**Abstract** The South China Sea (SCS) is a hydrographically complex and physically dynamic marginal sea of great economic importance. Primary production in the SCS experiences strong seasonal forcing through the monsoon cycle, which affects both riverine runoff and circulation within the basin. The summer monsoon in particular produces a mix

Handling editor: Judit Padisák

**Supplementary Information** The online version contains supplementary material available at https://doi.org/10.1007/s10750-023-05290-8.

L. Nguyen-Ngoc (☒) · H. Doan-Nhu Institute of Oceanography, Viet Nam Academy of Science and Technology, Nha Trang, Khanh Hoa, Viet Nam e-mail: ngoclam-ion@planktonviet.org.vn

Present Address:

S. C. Weber

Department of Biology, University of Southern Denmark, 5230 Odense, Denmark

S. C. Weber · M. Voss Biological Oceanography, Leibniz Institute for Baltic Sea Research Warnemünde, 18119 Rostock, Germany

A. Subramaniam Lamont-Doherty Earth Observatory at Columbia University, Palisades, NY 10964, USA

J. P. Montoya (⋈) School of Biological Sciences, Georgia Institute of Technology, Atlanta, GA 30332, USA e-mail: montoya@gatech.edu and symbiont. **Keywords** South China Sea · Diatom-Diazotroph Associations · Mekong River · Upwelling · Richelia intracellularis · Calothrix rhizosoleniae · Chaetoceros compressus

of waters affected by the Mekong outflow and coastal

upwelling embedded within a dynamic wind-driven

surface circulation. Here, we discuss the distribution,

abundance, and symbiotic state of a suite of host dia-

toms and Diatom-Diazotroph Associations (DDAs) in

different habitats defined in terms of the physical and

biological characteristics of the SCS during the early stages of the SW Monsoon of 2016. DDA host diatoms were broadly distributed throughout our study

region, and we found intact symbioses in all of the habitats sampled, though infection rates (abundance

of hosts bearing symbionts) and infection intensities

(number of symbionts per host) were lowest in waters affected by coastal upwelling. Host infection rates

tended to be highest in offshore waters, and DDA host

diatoms generally varied widely in size and infection

intensity both within and among defined habitats. These differences may reflect different optimal strate-

gies for allocating biomass and energy between host

#### **Abbreviations**

DDAs Diatom-Diazotroph Associations

MLD Mixed layer depth MRW Mekong River habitat NAI Nitrate availability index



NE North east
OnSW Onshore water
OSW Offshore water
SCS The South China Sea
SSS Sea surface salinity
SST Sea surface temperature

SW South west UpW Upwelling habitat

zChlM Depth of the chlorophyll maximum

## Introduction

Nitrogen availability limits primary production in many parts of the ocean because the biological demand for combined forms of nitrogen (e.g., NO<sub>3</sub><sup>-</sup> and NH<sub>4</sub><sup>+</sup>) in the surface layer commonly exceeds the rate of supply by vertical mixing, atmospheric deposition, and other pathways that provide reactive nitrogen to surface waters (Gruber & Galloway, 2008). Under these conditions, organisms with the capacity to use dissolved N<sub>2</sub> as a substrate for growth, known as N<sub>2</sub>-fixers or diazotrophs, have a selective advantage and can grow and produce biomass as long as other essential nutrients are available (e.g., Ward et al., 2013; Follett et al., 2018).

A diverse array of prokaryotes are capable of diazotrophic growth and N<sub>2</sub>-fixation is the dominant pathway injecting combined nitrogen into the ocean system (e.g., Zehr & Capone 2020). In many regions, particularly tropical systems affected by large riverine inputs, symbiotic associations between diatoms and diazotrophic cyanobacteria (Diatom-Diazotroph Associations, or DDAs) are abundant and highly active (see review by Paerl et al., 2008), often forming dense blooms that support very high rates of N<sub>2</sub>- and CO<sub>2</sub>-fixation (Capone et al., 2005; Marconi et al., 2017). In these symbioses, the hosts are typically centric diatoms of the genera, Rhizosolenia, Hemiaulus, and Chaetoceros, while the common symbionts are heterocystous filamentous cyanobacteria of the genera Richelia and Calothrix (Heinbokel, 1986; Villareal, 1989; Foster et al., 2010). Studies in the Western Tropical North Atlantic have shown a strong association between the Amazon Plume and the growth and activity of DDA populations (Subramaniam et al., 2008; Goes et al., 2014; Weber et al., 2017), which is likely mediated by nutrient transport and mixing associated with the river plume and its margins. These factors are likely to promote DDA growth in other tropical river-ocean systems, though considerable uncertainty remains about the ways in which nutrient availability and mixing of riverine and oceanic waters may interact to control DDA growth (Follett et al., 2018). Epithemia (Diatoms) also contains diazotrophs has been found in the subtropical North Pacific Ocean by Schvarcz et al. (2022).

The SCS is one of the world's largest marginal seas, covering some 3.5 million km<sup>2</sup>. The waters of the SCS are strongly affected by the annual monsoon cycle, which have a strong impact on both circulation within the basin and land-ocean coupling through riverine runoff. The winter monsoon (Oct-Mar) blows from the northeast and drives a basin-wide cyclonic circulation cell (Wyrtki, 1961) which suppresses upwelling off the coast of Viet Nam. In contrast, the summer, or Southwest (SW), Monsoon (Jun-Sep) creates two circulation cells within the SCS with an offshore jet at about 12° N on the Vietnamese coast (Wu et al., 2003; Dippner et al., 2007, 2011). Coastal upwelling along the Vietnamese coast brings to the surface high salinity waters of North Pacific origin (Liu et al., 2010) during the SW Monsoon, supporting high rates of primary production (Nguyen, 1997; Dippner et al., 2007).

In addition to their effects on coastal upwelling and basin circulation, the monsoons bring intense rainfall to Indochina, which in turn drives large pulses of riverine flow into the SCS via the Mekong River (Shaw & Chao, 1994). The Mekong River is the ninth largest in the world with an annual discharge of 470 billion m<sup>3</sup>. The path of the Mekong outflow differs between seasons, tending to form a southward coastal jet during the winter or NE monsoon and spreading northwards over the shelf during the summer or SW monsoon. This creates an interesting spatial juxtaposition of nutrient inputs via coastal upwelling and riverine runoff during the summer monsoon. Both upwelling and the Mekong River are responsible for nutrient supply and impact nitrogen fixing species. During the monsoon season when the river outflow was particularly strong, nitrogen fixation was up to ten times higher than during the intermonsoon period (Voss et al., 2006). More recently, Grosse et al. (2010) suggested that DDAs may play an important role near the river mouth but these details were not studied in the entire coastal waters off Viet Nam. Diatoms can be strongly supported by symbiont



hosts like the cyanobacterium *Richelia intracellula- ris* J.Schmidt and develop strong blooms in tropical oceans (Villareal et al., 2011). Such associations play an important role in the export of carbon to the deep ocean in waters affected by the riverine input of the Amazon (Subramaniam et al., 2008). However, the conditions and ways in which different water mass constituents contribute to the development and persistence of these symbiotic associations are not yet well understood.

Here we present data on the distribution, abundance, and symbiotic state of a suite of host diatoms and DDAs in Vietnamese waters of the SCS during the earliest stages of the SW Monsoon of 2016. We assess these floristic measurements in the context of the complex hydrography of the region to characterize the factors that promote growth of DDAs, biogeochemically important members of the plankton community, and to explore the plasticity of the symbiotic associations in a dynamic, hydrographically variable region.

## Materials and methods

Hydrographic data and nutrient samples

Samples were collected during cruise FK160603 aboard the R/V Falkor (3–19 June 2016). Our cruise track sampled diverse waters, including offshore waters of the South China Sea, shelf waters, shelf waters influenced by the Mekong River outflow, and the coastal upwelling zone around 12° N (Fig. 1). Stations were chosen using a combination of real-time shipboard measurements of surface T and S and satellite measurements of SST, Chla, and Kd<sub>490</sub>, a proxy for salinity in this region.

Water samples and hydrographic data were collected using a SBE-911 CTD and a rosette equipped with twenty-four 10 l bottles. Nutrient samples  $(NO_3^- + NO_2^- \ [N+N], \ PO_4^{3-}, \ SiO_2)$  were filtered through 0.2 µm cellulose acetate filters, then frozen at sea and analyzed ashore using a Lachat QuikChem 8000 flow-injection analysis system. The precision of the nutrient measurements were 0.02 µM, 0.01 µM and 0.3 µM, respectively. In the lab, samples were thawed, then equilibrated at room temperature for at least 24 h prior to analysis. The deviation in the ratio of nitrate to phosphate from Redfield stoichiometry

was calculated using the method outlined in Gruber & Sarmiento (1997).

Phytoplankton community measurements

We characterized the phytoplankton community by microscopic identification and enumeration. At a typical station, we used the CTD-rosette to sample six depths in the upper 100 m of the water column including the mixed layer, the pigment maximum, and other features of interest. At nearshore stations where the water column depth was less than 100 m, we sampled to about 5 m above the sea floor. Every cast is identified by a numeric string SSS.EE, where SSS is the station number and EE is an event number assigned sequentially to each sampling operation at a station. Thus, 001.04 identifies the fourth sampling event at Station 001.

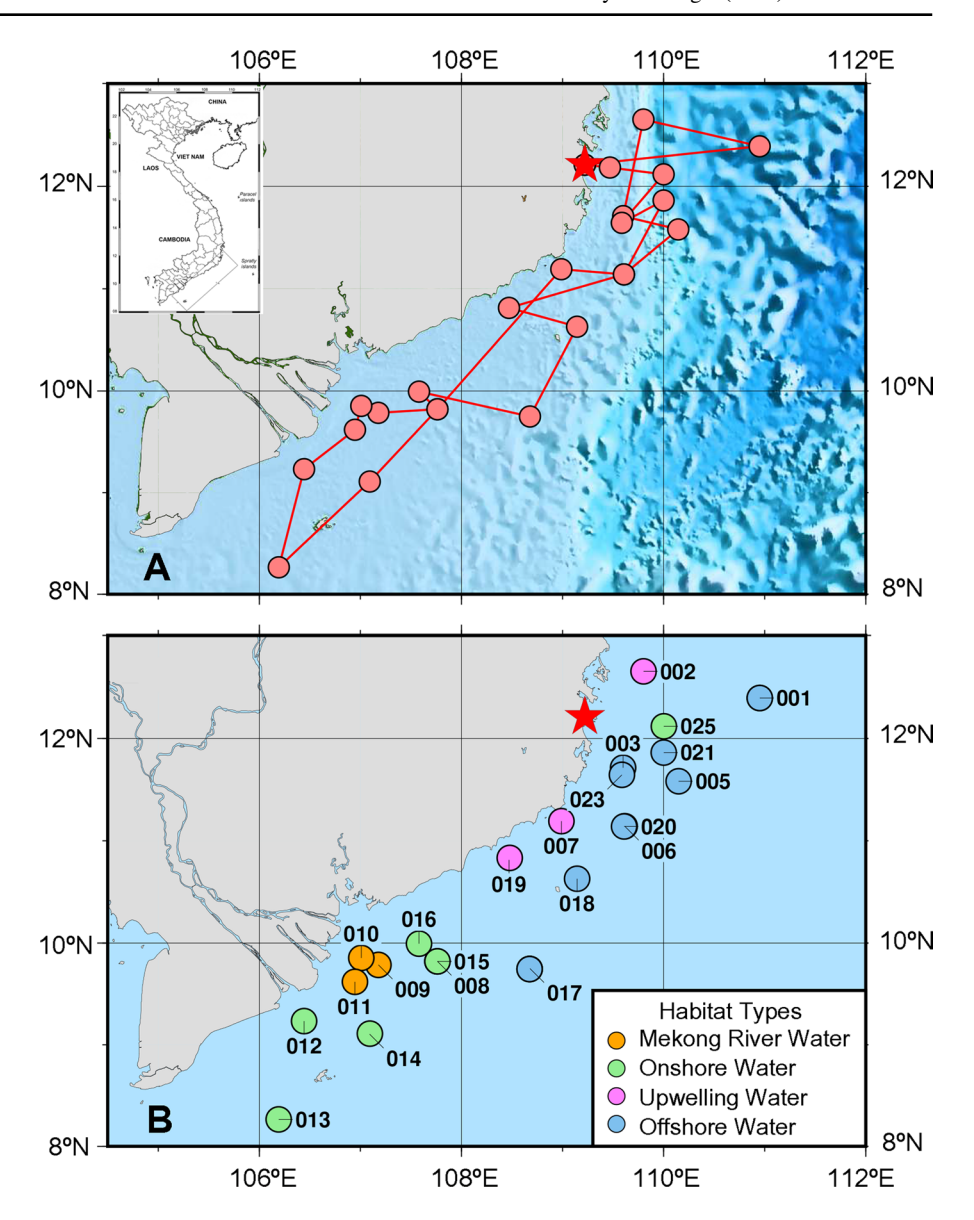
At each depth sampled, 1.5 l of water was transferred to a plastic bottle, fixed with Lugol's solution (5% final concentration), then stored under cool, dark conditions for processing ashore. In the laboratory, the samples were concentrated by gravitational settling in a graded series of cylinders (1000, 100, and 15 ml). Each settling step required a settling time of > 48 h, after which the supernatant was removed before further settling (first two steps) or transferred to a 15 ml polypropylene centrifuge tube (CLS430791 Sigma, Corning®) for storage. The final settling stage produced a sample with a volume of 2–5 ml for microscopic counting. We recognize that epiphytic symbionts might be lost during our handling and processing of samples; thus, our measurements provide a lower limit to their abundance.

Phytoplankton in CTD-rosette samples were enumerated at the species level using a Sedgwick-Rafter counting chamber and an Olympus CX41 microscope (× 100 magnification). At least 300 cells were counted from each sample to produce an estimated counting error of 11.5%.

In addition to the discrete samples from specific depths, we collected vertically integrated plankton samples in vertical tows (100 m to the surface) of a Juday net (45 µm mesh). These samples provided sufficient material for statistically robust enumeration of DDAs and characterization of the symbiosis (rate of association and number of symbionts per host cell). Net samples were fixed with neutral Lugol's solution (5% final concentration) and stored in dark bottles



Fig. 1 Track and major stations sampled during cruise FK160603 (A) and stations coded by habitat type (B): MRW = orange, OnSW = green, UpW = purple, OSW = blue



(500 ml) at room temperature. Samples were concentrated by settling in the laboratory in 500 ml cylinders and the final concentrated sample was stored in 30 ml bottles. After species enumeration, formaldehyde solution was added to the samples (4% to final concentration) for long-term storage.

Net plankton samples were examined using a Leica LDMB microscope with phase contrast (PC) and differential interference contrast (DIC) optics, and equipped with an epifluorescence unit. Host cells were identified and characterized under PC and DIC illumination. Cyanobacterial symbionts (*Richelia intracellularis* and *Calothrix rhizosoleniae* Lemmermann) were identified and characterized (e.g., size, shape, numbers of heterocysts, number of trichomes) using their pigment autofluorescence under blue light excitation. A digital camera, Olympus DP71, was used for microphotography.

Standard references were used for identifying species of *Rhizosolenia, Chaetoceros*, and *Hemiaulus*, including the works by Sundström (1986), Round et al. (1990), Tomas (1997), and Doan-Nhu et al. (2014). Validation of scientific names followed Guiry (2020).



# Habitat types

To explore the association between environmental factors and the distribution and abundance of DDAs, we used the habitat type definitions of Weber et al. (2019) for this cruise. In this approach, stations were characterized using a Principal Components Analysis (PCA) and Hierarchical Cluster Analysis (HCA) of a suite of surface and profile-based properties, including sea surface temperature (SST), SSS, mixed layer depth (MLD), depth of the chlorophyll maximum (zChlM), and a nitrate availability index (NAI). The NAI is a nondimensional parameter designed to capture the impact of nutrient availability on phytoplankton communities and was defined as:

- a. [N+N] when surface  $[N+N] \ge 0.5 \mu M$ , with N+N meaning the summed concentrations of  $NO_3^- + NO_2^-$
- b. The depth at which [N+N] reached 2  $\mu$ M when surface [N+N] < 0.5  $\mu$ M
- a. Deepest depth at shallow stations where surface [N+N] < 0.5  $\mu$ M and [N+N] never reached 2  $\mu$ M at depth.

## Results

# Hydrography and habitat types

The analysis of Weber et al. (2019) provided a robust, biologically relevant grouping of our stations into four major habitat types. Mekong River Water stations (MRW) were characterized by warm, fresh water at the surface and were all in shallow waters near the mouth of the river. Stations clearly affected by coastal upwelling (UpW) were found closer to the shoreline in the northern portion of our sampling area. These stations had colder, saltier waters at the surface, shallow MLDs, and variable zChlM and measurable surface N+N concentrations. The remaining shelf stations fell into a group named OnSW, which was characterized by moderate surface water T and S, very low surface N+N concentrations, and moderate MLDs. Finally, our offshore stations formed a clear oceanic group (OSW), which was very similar to the OnSW group in surface water properties, but had characteristically deep mixed layers and chlorophyll maxima. Figure 1 shows our track, station locations,

and the habitat types defined for our major stations by Weber et al. (2019). In addition, distribution of chlorophyll-*a* is presented in Figure S1.

Surface concentrations of phosphate and silicate were highest at MRW stations and both ions were present in measurable concentration at the surface at all stations sampled (Fig. 2A, C). In contrast, surface N+N concentrations were low ( $<0.5 \mu M$ ) at most stations, though we found higher concentrations at some of the MRW and UpW stations (Fig. 2B). The ratio of N+N to phosphate concentrations in surface waters was generally well below the Redfield Ratio, with negative  $N^*$  (Gruber & Sarmiento, 1997) values at most stations, implying strong nitrogen limitation. These conditions are often interpreted as optimal for the occurrence of nitrogen fixing cyanobacteria (Gruber, 2019), but it is also widely know that this is not always the case (Mulholland et al., 2019). Interestingly, the MRW stations all showed very low N\* values below  $-2 \mu M$ , while the other three habitats had mean  $N^*$  values around – 1  $\mu$ M (Fig. 2D).

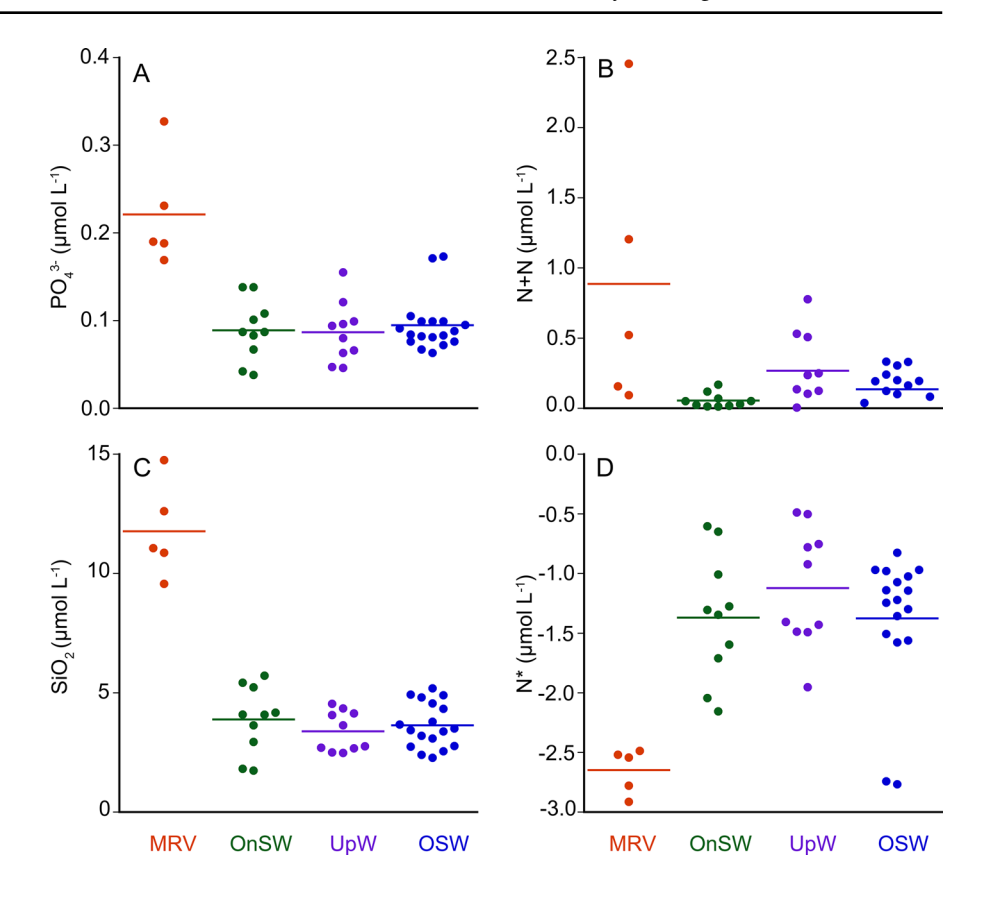
DDA diversity, abundance, and infection rates

We found seven distinct DDA host species in these waters during cruise FK160603 (Table 1). The most abundant and widely distributed diatom hosts were Chaetoceros compressus Lauder (Fig. 3A-C), and Hemiaulus membranaceus Cleve (Fig. 3C, E), both of which were found throughout our work area. A third host species, Rhizosolenia clevei var. communis Sundström (Fig. 3G-I), was also broadly distributed but was absent from the southern part of our work area as well as the core of the coastal upwelling region. H. membranaceus and Rhizosolenia clevei var. communis form DDAs with Richelia intracellularis, while C. compressus associates with epiphytic Calothrix rhizosolenia. Other DDAs were found only at one or a few stations and involved R. intracellularis associated with the host diatoms Rhizosolenia clevei Ostenfeld (Fig. 3K, L), Guinardia cylindrus (Cleve) Hasle (Fig. 3M, N), Hemiaulus chinensis Greville, Hemiaulus indicus Karsten (Fig. 3O, P), and Hemiaulus hauckii Grunow ex Van Heurck (Fig. 3Q).

Host diatom and DDA abundances varied widely (Figs. 4, 5), with cell concentrations as high as 5000–6000 cells 1<sup>-1</sup> (*H. chinensis*, Stn. 016.03). Among the broadly distributed DDA host diatoms, *R. clevei* var. *communis* occurred at maximal densities of



Fig. 2 Surface concentrations of phosphate (A), nitrate+nitrite (B), silicate (C), and  $N^*(D)$  in each habitat type during cruise FK160603. Horizontal lines show the mean values for each habitat type. Colors as in Fig. 1



375 cells  $1^{-1}$ , *H. membranaceus* reached 965 cells  $1^{-1}$ , and *C. compressus* attained densities of 1502 cells  $1^{-1}$ . The areal abundances (cells  $m^{-2}$ ) of the widely distributed host diatoms varied with habitat type, in part as a result of the different integration depths (Table 1, Fig. 6). These vertically integrated host diatom and DDA abundances were highest in offshore waters, ranging as high as  $3.9 \times 10^7$  cells  $m^{-2}$  for *C. compressus* and  $2.5 \times 10^7$  cells  $m^{-2}$  for *H. membranaceus* (Figs. 5, 6, Table 1).

At each station, the symbiont infection rate (infection intensity) for each diatom host was determined through counts of diatoms collected in vertical net tows extending to 100 m depth or 5 m above the bottom at shallow stations where the maximum depth was less than 100 m. Infection rate varied widely among host diatoms as well as spatially, ranging from 0 to 100% of host cells bearing at least one symbiont (Fig. 6). In general, *C. compressus* was the host most likely to be uninfected across all habitat types, while *H. membranaceus* was the least likely of the widely distributed diatoms to be symbiont free (Fig. 5).

The nature of symbiont infection also varied widely both among hosts and habitat types (Fig. 7). The most obvious difference was in the number of symbionts per host cell, which reached as high as 12 symbionts in a single cell of R. clevei (not shown). The three most widely distributed DDAs (C. compressus, H. membranaceus, and R. clevei var com*munis*) showed distinct patterns of infection intensity. The association between Chaetoceros compressus and epiphytic Calothrix rhizosoleniae was the weakest, though its frequency was potentially underestimated by our methods, which may have dislodged loosely associated epiphytes. We found frequent instances of uninfected hosts, and most infections involved only a single symbiont per host cell. In contrast, the most common infection pattern for H. membranaceus was two R. intracellularis per host cell, though singly infected hosts occurred regularly in Upwelling and Offshore Waters (Fig. 6). The two relatively large diatoms Rhizosolenia clevei var. communis and G. clvindrus showed the most intense association with Richelia intracellularis, with most diatom cells supporting



**Table 1** DDA host abundances and infection rates in different habitat types

Habitat type/DDA	Abundance (10 <sup>3</sup> cells m <sup>-2</sup> )		Infection rate (%)	
	Minimum	Maximum	Minimum	Maximum
Mekong river water (integration depth	: 20–26 m)			
Chaetoceros compressus	< 10	2700	0	0
Hemiaulus membranaceus	1500	5500	88	94
Rhizosolenia clevei var. communis	630	2800	88	100
Hemiaulus indicus	< 10	1500	50	50
Guinardia cylindrus	< 10	< 10	100	100
Rhizosolenia clevei	< 10	< 10	100	100
Hemiaulus hauckii	< 10	1100	ND	ND
On-shelf Water (integration depth: 28-	-34 m)			
Chaetoceros compressus	360	11,000	0	73
Hemiaulus membranaceus	< 10	13,000	17	100
Rhizosolenia clevei var. communis	< 10	3,600	74	100
Hemiaulus indicus	< 10	5,500	0	0
Guinardia cylindrus	< 10	1,600	25	100
Rhizosolenia clevei	< 10	< 10	100	100
Hemiaulus hauckii	< 10	7300	ND	ND
Upwelled Water (integration depth: 27	′–100 m)			
Chaetoceros compressus	< 10	1900	0	50
Hemiaulus membranaceus	< 10	4800	25	100
Rhizosolenia clevei var. communis	< 10	< 10	0	100
Hemiaulus indicus	< 10	< 10	100	100
Guinardia. cylindrus	< 10	< 10	50	100
Rhizosolenia clevei	< 10	< 10	100	100
Hemiaulus hauckii	< 10	1900	ND	ND
Oceanic Seawater (integration depth: 8	35–106 m)			
Chaetoceros compressus	< 10	39,000	0	50
Hemiaulus membranaceus	110	25,000	17	100
Rhizosolenia clevei var. communis	< 10	7900	81	100
Hemiaulus indicus	< 10	180	17	100
Guinardia cylindrus	< 10	210	67	100
Rhizosolenia clevei	< 10	61	67	100
Hemiaulus hauckii	< 10	20,000	100	100

multiple symbionts and frequently hosting four or more symbionts in all habitat types (Fig. 6).

# DDA morphology

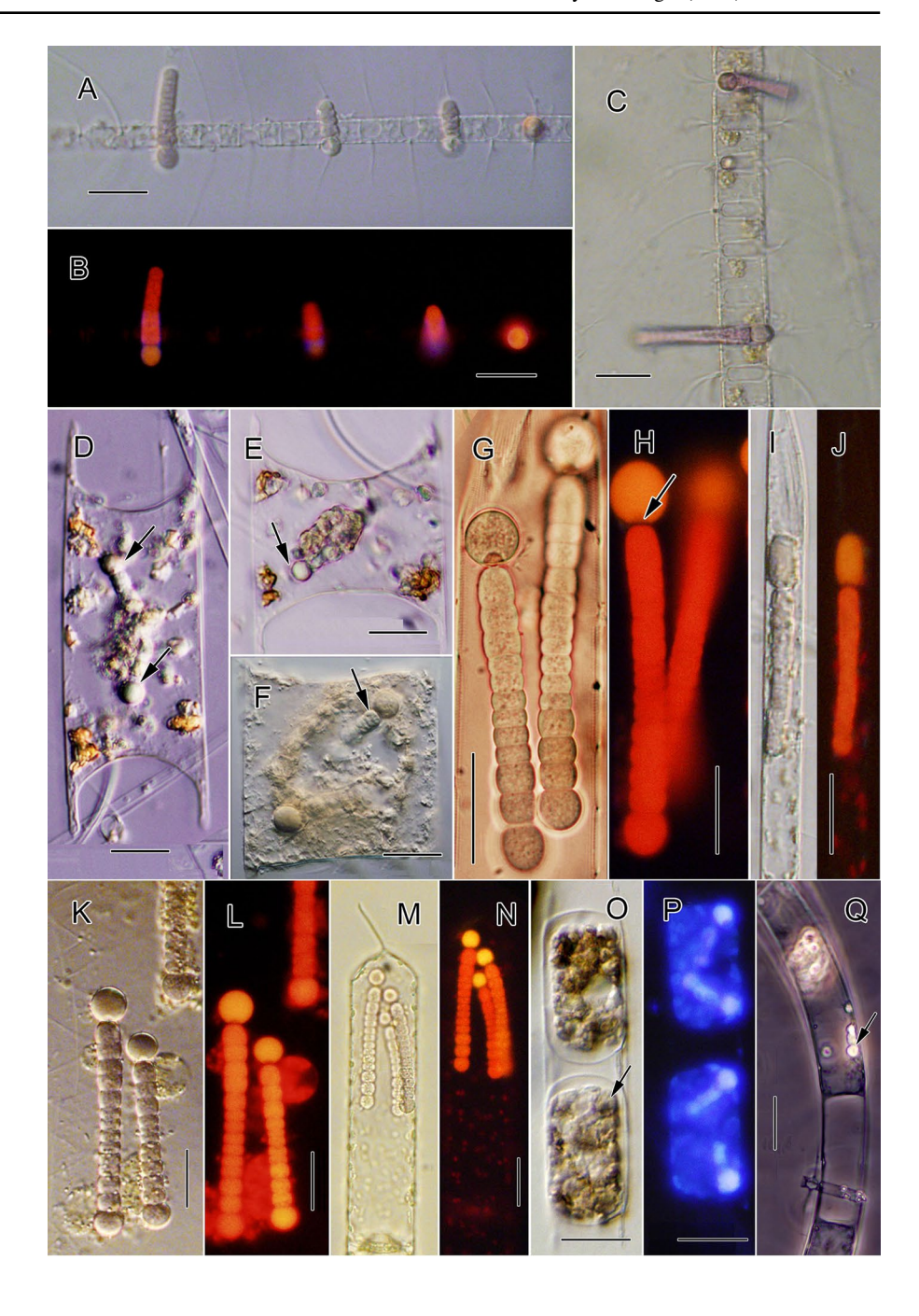
The cell volume of the abundant diatom hosts varied significantly both within and among species, though in general, cell volume did not show a consistent relationship with habitat type (Fig. 5). The primary exception was *C. compressus*, which showed a much greater range in cell volume in offshore waters (OSW) than in the other habitats (Fig. 5A). This

increased range appeared to involve distinct size classes of cells, a pattern that also appears in the size distributions of *R. clevei* var. *communis* (Fig. 5C) and *G. cylindrus* (not shown).

For the DDA community as a whole, we found a clear relationship between host cell volume and infection intensity, or the number of symbionts per host cell. For *Rhizosolenia* spp., this relationship was driven strongly by the large size contrast between the smaller *R. clevei* var. *communis* and the much larger *R. clevei* (Fig. 7). The slope of the relationship between infection intensity and host cell volume was



Fig. 3 Images of the three most widely distributed DDAs sampled during cruise FK160603. Heterocystous cyanobacteria Calothrix rhizosoleniae epiphytic on the chain diatom Chaetoceros compressus under DIC (A, C) and EPI (B) optics; Colonies of R. intracellularis with heterocysts (arrows) inside the frustule of Hemiaulus membranaceus under PC (**D**, **E**) and DIC optics (**F**); Colonies of Richelia intracellularis in the common host diatom Rhizosolenia clevei var. communis under PC (G) and EPI (H) optics; Colonies of R. intracellularis in the host diatom Rhizosolenia hebetata under DIC (I) and EPI (J) optics; Colonies of the heterocystous cyanobacteria Richelia intracellularis associated with Rhizosolrnia clevei under DIC (K) and EPI optics (L); R. intracellularis assocated with Guinardia cylindrus under PC (M) and EPI (N) optics; R. intracellularis (arrow) inside H. indicus under DIC (O) and EPI (P) optics; R. intracellularis (arrow) inside H. haucki under PC (Q) optics. All scale bars =  $20 \mu m$ . PC phase contrast optics, DIC differential interference contrast optics, EPI epifluorescence illumination



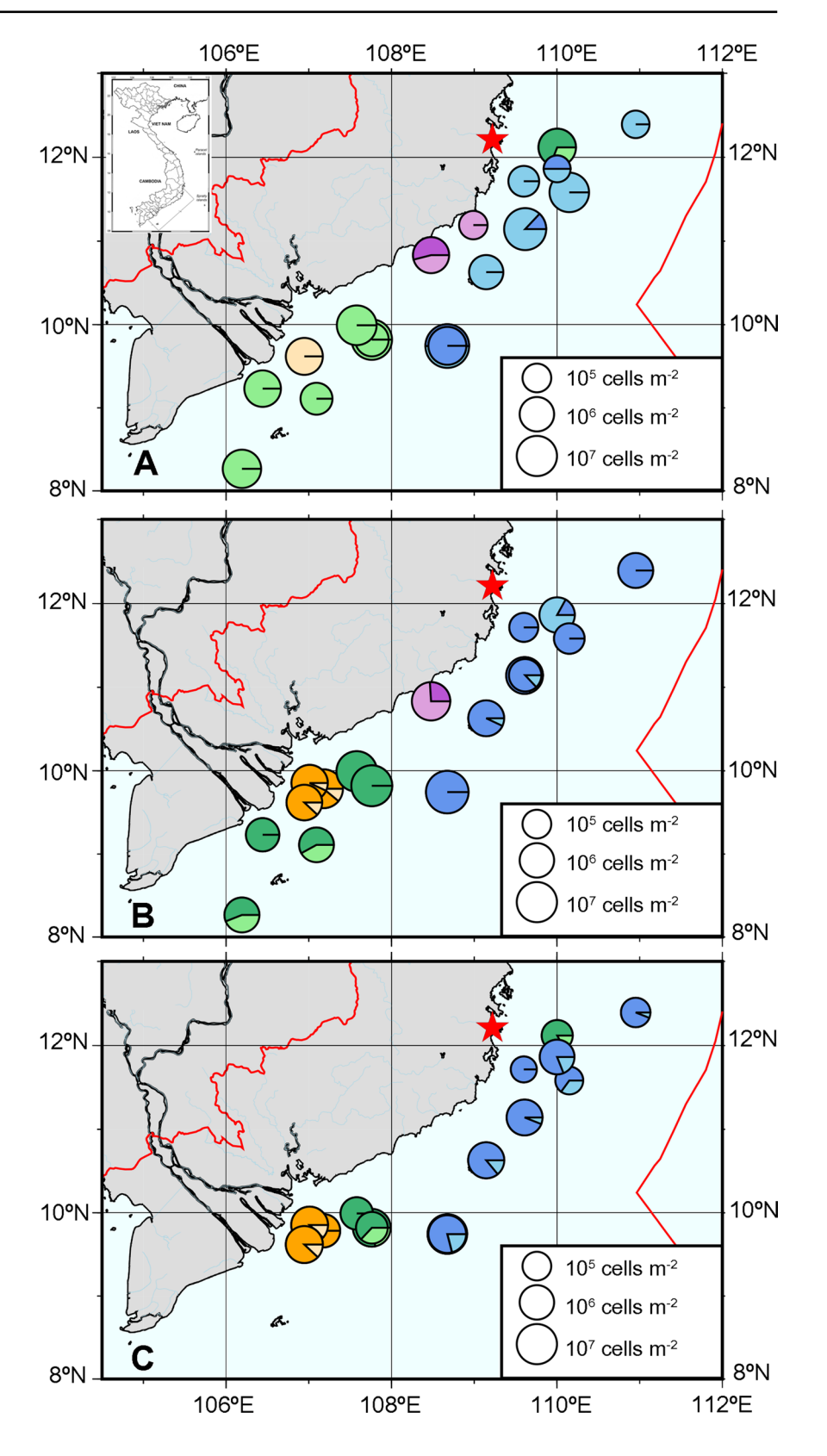
steeper for smaller species, *R. clevei* var. *communis* and *G. cylindrus*, than for the larger *R. clevei*. Interestingly, the slope of this relationship scaled inversely with host size for these three species.

The cyanobacterial symbionts also varied in morphology, though they uniformly had a single terminal heterocyst (Fig. 3A, C, E, F, G, K, M). In general, the chains of *Calothix rhisosoleniae* epiphytic on *C*.

compressus and chains of Richelia intracellularis endosymbiotic in Hemiaulus spp. were shorter and smaller in size than the symbionts associated with R. clevei var. communis (Fig. 3). The smaller symbionts were often hard to visualize, but their heterocysts were clearly visible under phase contrast and differential interference contrast optics (Fig. 3D–F). Almost all heterocysts were globular with a polar nodule,



Fig. 4 Abundance and symbiont infection rate of the three most widely distributed diatom hosts sampled during cruise FK160603, C. compressus (A), H. membranaceus (B), and R. clevei var. communis (C). Circle areas are proportional to the areal abundance of diatoms (cells m<sup>-2</sup>), and the dark wedges represent the proportion of the host population at each station carrying one or more symbionts. Colors as in Fig. 1: MRW = orange, OnSW = green, UpW = purple, OSW = blue





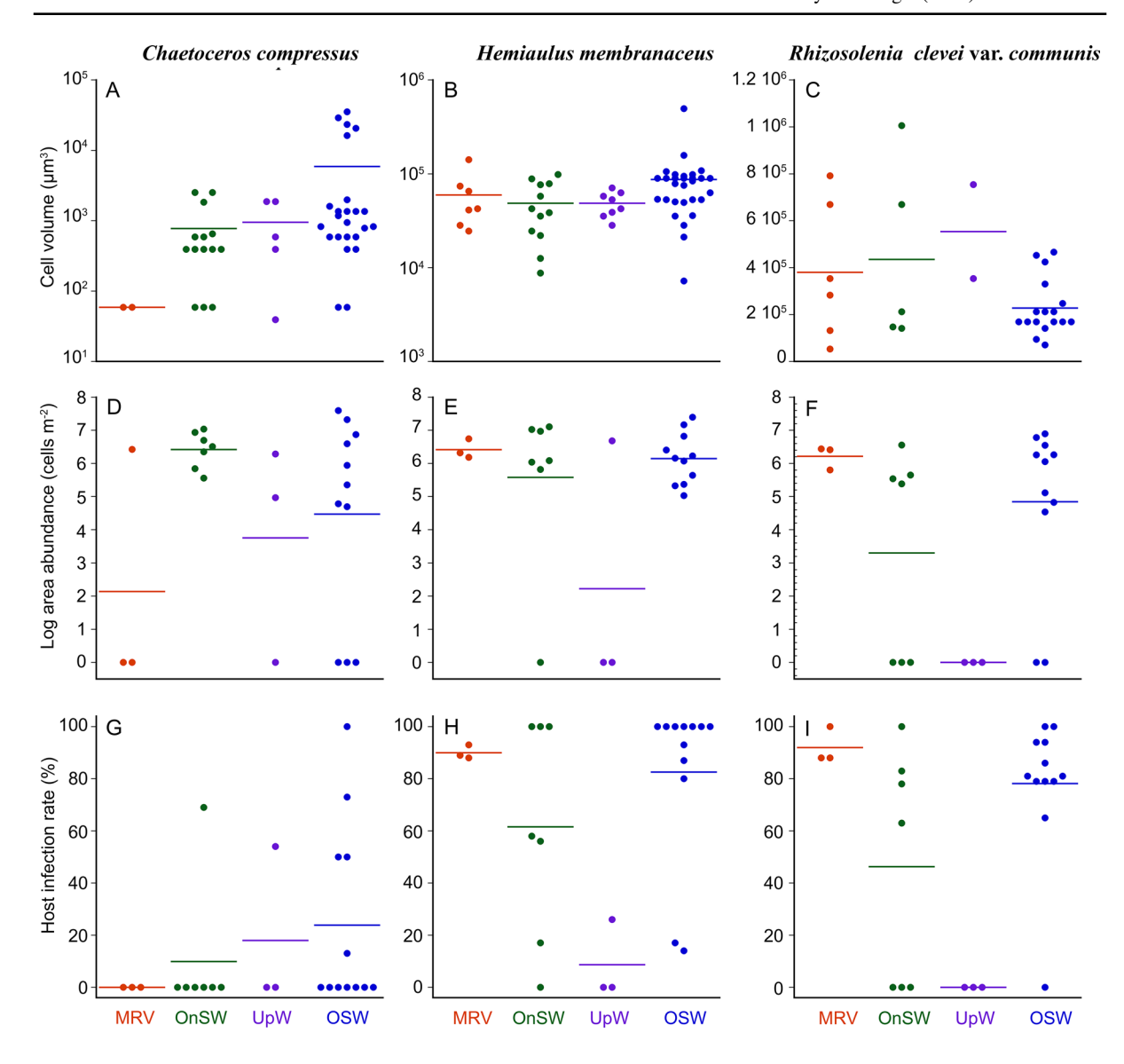


Fig. 5 Summary of host diatom volume (A–C), DDA host diatom abundance (D–F), and host infection rate (G–I) in different habitat types for the three most widely distributed DDAs

sampled during cruise FK160603. Horizontal lines show the mean values for each habitat type

which distinguished them from the hemispherical, generally enlarged cells at the other end of the chain (Fig. 3G, H, K, L).

The average number of cells in chains of *Richelia intracellularis* in *R. clevei* var. *communis* was  $12\pm3$  cells (range 6–20, n=82), and colonies with 11 cells accounted for 21% of the symbiont population (Fig. 8). The size of symbiont colonies in *Hemiaulus* spp. and *R. clevei*, as well as the epiphytes on *C. compressus* was not measured due to their

very short chains and the difficulty of imaging them microscopically.

### Discussion

The dynamic habitat delineation which we applied was first described by Weber et al. (2019) and is based on the same hydrographic and physical data set. Most important for the definition of habitats where



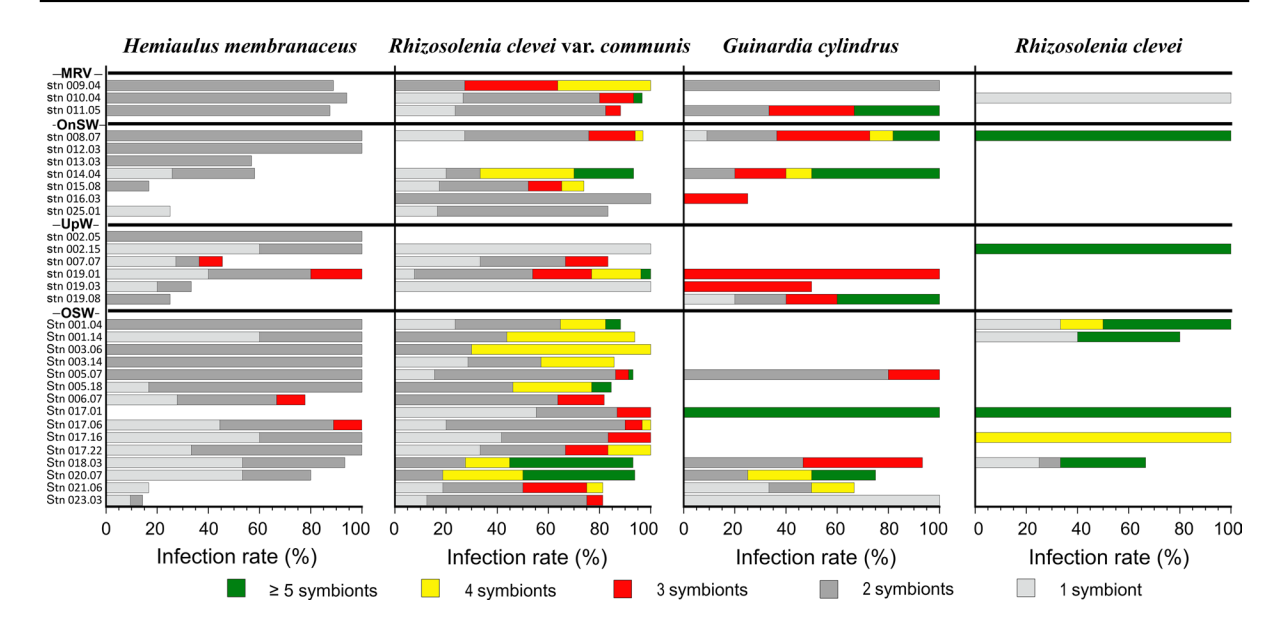
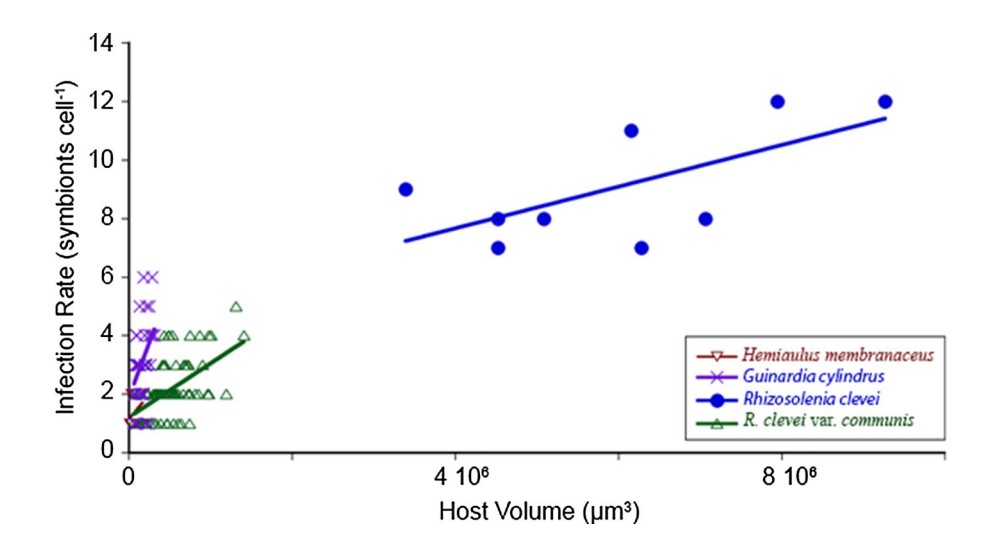


Fig. 6 Infection intensity for hosts with high variation in number of symbionts per host cell during cruise FK160603. Stations are grouped by water type and horizontal bars reflect overall infection rate subdivided by infection intensity

Fig. 7 Infection intensity as a function of host size in DDAs that show high variation in number of symbionts per host cell. Least square lines of regression show trends within each species; note that the slopes generally decrease as host size increases



MLD, depth of Chl maximum and the NAI. The MRW stations were all closely related to the Mekong River plume and had a shallow MLD and high NAI as well as warm surface waters. The open sea stations (OSW), had a very low NAI and deep Chl maximum. The three upwelling stations (UpW) were all located near the coast and were far away from the river mouth. They were characterized by shallow MLD and higher nutrient availability while the OnSW stations were mostly further away from the Mekong River

mouth and show little impact of both the river and upwelling processes.

During the early phase of the SW Monsoon, the South China Sea is a dynamic environment with phytoplankton communities shaped by multiple physical and biogeochemical forcings. Sampling was performed in a post-ENSO year with a weak south west monsoon and low discharge of the Mekong River (Ha et al., 2018) It is difficult to clearly distinguish the river plume from the Mekong/Gulf of Thailand



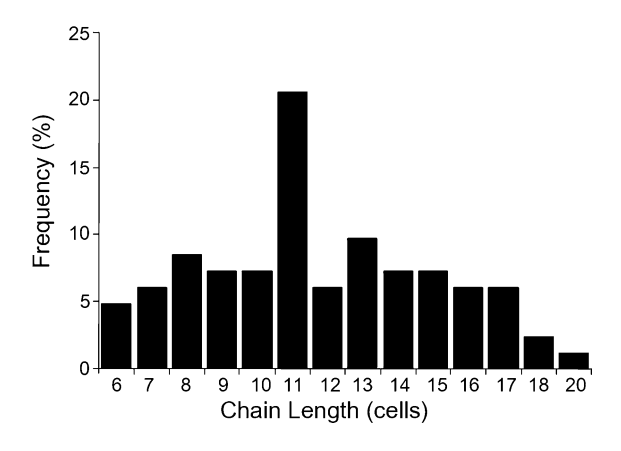


Fig. 8 Frequency distribution of *Richelia intracellularis* chain length in *Rhizosolenia clevei* var. *communis* 

waters, that enter the study area from the south and previous studies have often used salinity with unclear results for the distinction (Voss et al., 2006, 2014; Grosse et al., 2010; Loick-Wilde et al., 2017). The multivariate analysis of Weber et al. (2019) provides a robust framework for exploring the factors that regulate the abundance and diversity of phytoplankton in this heterogeneous environment. In general, we found appreciable concentrations of DDAs in all regions of our work area, while the abundance of specific host diatoms and their infection rates varied among habitats. For example, R. clevei var. communis was largely absent from waters affected by coastal upwelling (UpW habitat), and both H. membranaceus and C. compressus abundances were relatively low in this habitat in comparison to onshore and offshore waters (Fig. 5). In contrast, C. compressus was found at only one of the three Mekong River Water (MRW) stations, where it had an infection rate of zero. In general, infection rates for the three common DDAs were highest in OSW, though *H. membranaceus* and R. clevei var. communis showed high infection rates in MRW. For all three common DDAs, low infection rates were associated with UpW.

Host infection rate varied among the different associations and habitat types sampled in our study (Figs. 4, 5), a pattern that contrasts with prior findings in the Western Tropical North Atlantic (Foster et al., 2007) and Eastern Equatorial Atlantic (Foster et al., 2009). This may reflect the relatively small scale and strong spatial gradients of the South China Sea in comparison to many other systems. For example, our

work area covered about 140,000 km² extending over only some 6° of longitude and about 4° of latitude. In this relatively small oceanographic area, 4 distinct habitats with clearly different physical characteristics were found (Weber et al., 2019); from estuarine water masses to an upwelling area. In contrast, the waters of the Western Tropical North Atlantic influenced by the Amazon Plume extend over at least 10° of longitude and 10°–15° of latitude, with an areal extent greater than 900,000 km². The scale of variation in our South China Sea data could easily be missed in a study designed to resolve spatial patterns in the much larger Amazon Plume region.

#### DDA distribution in the South China Sea

Our nutrient measurements show measurable, and at times high concentrations of phosphate and silicate in surface waters at all stations (Fig. 2). In contrast, the concentration of N+N was quite low at many of our stations, and the molar N:P ratio in dissolved nutrients was well below the canonical Redfield value of  $\sim 16:1$ , as reflected in the generally negative  $N^*$ values throughout our study region (Fig. 2D). Low N\* values imply nitrogen limitation of production, conferring a selective advantage on N2-fixing organisms. In the case of DDAs, the cyanobacterial symbiont is diazotrophic and can relieve nitrogen limitation by providing the association with access to the very large pool of dissolved N2. The diatom host in the association has a constitutive silicon requirement, so the abundant silicate (Si:N generally>>1:1) and phosphate in combination with low concentrations of N+N in surface waters of the SCS (Fig. 2) provide an environment where DDAs can outcompete other, non-diazotrophic phytoplankton (Subramaniam et al., 2008; Goes et al., 2014; Weber et al., 2017).

Two of the three most common diatom hosts in our study, *H. membranaceus* and *R. clevei* var. *communis*, were associated with the colonial cyanobacterium *Richelia intracellularis*, which is known to associate with a broad range of diatom hosts. The genus *Richelia* was created by Schmidt in 1901 (Guiry 2020) with the type species, *Richelia intracellularis*, which was found living in the cells of the diatom *Rhizosolenia clevei* var. *communis* (originally misidentified as *Rhizosolenia styliformis* in the inner part of the Gulf of Siam near Koh Kram and the Malacca Strait. Ostenfeld (1902), later found this species



living symbiotically in both R. clevei var. communis and R. clevei var. clevei also near Koh Chang and Ko Kram. More recently, Sundstrom (1984) found Richelia intracellularis in many different diatom hosts, including Rhizosolenia clevei var. clevei, R. clevei var. communis, Hemiaulus hauckii, H. indicus, and H. membranaceus in both the Indian Ocean and the Caribbean Sea. A large number of other studies have documented the association of R. intracellularis with a broad range of diatom species in diverse waters around the world (Sournia, 1970; Venrick, 1974; Kimor et al., 1978; Sundstrom, 1984; Heinbokel 1986). In the South China Sea, Richelia intracellularis has been documented previously by Hoang (1962) and Pham (1969) in Vietnamese waters and by Gomez et al. (2005) in Indonesian waters. R. intracellularis is a promiscuous symbiont but can associate strongly with its host diatom, as evidenced by the high infection rates seen for H. membranaceus and R. clevei var. communis Sundström across a range of habitat types in the South China Sea (Figs. 4, 5, Table 1). This conclusion is reinforced by the frequent occurrence of multiply infected host cells carrying two or more symbionts as well as the genomic streamlining recently reported in *Richelia* (Caputo et al., 2018).

The third widely distributed diatom host in our data set, Chaetoceros compressus, formed associations with epiphytic Calothrix rhizosoleniae. Calothrix rhizosoleniae was first described by Lemmermann (1899) as a symbiont of the diatom Rhizosolenia in the Indian Ocean and later found in the Pacific Ocean near Hawaii (Lemmermann 1905). Although misidentified as Richelia, this species was also reported from Japan living epiphytically on C. compressus (Okamura 1907) and the Indian Ocean as an epiphyte of Chaetoceros contortus F.Schütt (Karsten 1907), though this report is complicated by confusion at the time between the two species Chaetoceros contortus and C. compressus (see details in Doan-Nhu et al., 2014). The identity of the symbiont was definitively established by Villareal (1989), who used the morphology and figures in the original species description to verify that the cyanobacterium living epiphytically on diatoms of the genus Chaetoceros was actually Calothrix rhizosoleniae. More recently, Foster et al. (2010) used genetic evidence to reinforce Villareal's conclusions. In contrast to R. intracellularis, C. rhizosoleniae appears to form much looser associations with its host, with many host cells remaining free of infection and most infected hosts carrying only a single symbiont. This looser association is also consistent with the epiphytic nature of this association, and is reflected in the larger genome size and greater metabolic capabilities of this symbiont relative to *Richelia intracellularis* (Caputo et al., 2018).

All of the DDA symbionts we observed had a single terminal heterocyst (Fig. 3A-Q), and many also had an enlarged vegetative cell at the other end of the filament (Fig. 3G, H, K, L). Heterocysts were distinguished by their globular shape and the presence of a polar nodule. The polar nodules were used in identification of the heterocysts in cyanobacteria. It is a structure that contains cyanophycin granules which are thought to act as a nitrogen buffer that temporarilyy stores recently fixed nitrogen (Sherman et al., 2000). Terminal vegetative cells were also usually globular or occasionally hemispherical, creating a superficial resemblance to heterocysts. The absence of a polar nodule was definitive evidence that these cells were not true heterocysts, though they may have been partially differentiated protoheterocysts as described by Villareal (1989). Interestingly, our microscopic observations also revealed differences in heterocyst morphology in symbionts of Rhizosolenia spp.; the heterocysts of *Richelia intracellularis* colonies in thinner Rhizosolenia host cells tended to be distinctly ovoid rather than spherical (Fig. 3A, B, F, G in contrast to Fig. 3C, D, A-Q). Ovoid heterocysts will have a higher surface:volume ratio than spherical heterocysts, which may facilitate exchange of carbon and nitrogen with the host diatom (e.g., Inomura et al., 2020).

We found DDA host diatoms in all of the habitat types we sampled in the South China Sea (Figs. 4, 5). While the presence of DDA hosts, both infected and uninfected, in oligotrophic OSW waters is not surprising, their presence in the Mekong River (MRW) and coastal (OnSW) waters suggests that the host diatoms at least are able to grow under a broad range of physical and nutrient conditions, confirming the findings of Grosse et al. (2010) and Bombar et al. (2011). Interestingly, Detoni et al. (2022) recently reported very low DDA abundances from a survey of the South Atlantic using quantitative PCR to quantify nifH phylotypes. The factors that control diazotroph community composition may differ among ocean basins and/



or hemispheres, possibilities that can only be evaluated through much broader scale surveys of diazotroph abundances. The only habitat that appeared to be unfavorable for these diatoms was upwelling waters (UpW), where R. clevei var. communis was absent and H. membranaceus was present at only one of three stations sampled. Although a persistent feature of the SW Monsoon in the South China Sea, coastal upwelling is episodic and contributes to both spatial and temporal variation in physical and biogeochemical conditions in the northern half of our sampling area. Stations in the UpW habitat had surface nutrient concentrations similar to those of other habitats, though N+N concentrations were a bit higher in upwelled waters (Fig. 2). The increased access to inorganic nitrogen in upwelled waters may promote growth of other, non-diazotrophic phytoplankton.

Finally, we found a range of host cell sizes in our data set, which may reflect physiological state and/or growth rate, though we did not find any clear association between habitat type and host size for any host other than *C. compressus*, which showed much greater variation in size in offshore waters than elsewhere. This may reflect the spatially and temporally heterogeneous nature of the South China Sea, with multiple sources of water contributing to the surface layer, e.g., Mekong water (MKGTW), mixed water mass 3 (WM3) and open sea waters (OSW) (Loick-Wilde et al., 2017), and physical forcings through local wind and larger scale advective processes leading to mixing on a wide range of temporal and spatial scales.

## DDA infection rate and intensity

In general, host infection rates tended to be higher in OSW than elsewhere (Fig. 4), though most species showed appreciable variation in infection rate in all habitats (Fig. 5G–I). Interestingly, most species showed high infection rates in the freshest waters sampled (MRW), suggesting that DDAs are both tolerant of lower salinities and that the associations can be established and maintained under the dynamic and variable physical conditions prevalent in and near river plumes. The Mekong outflow introduces nutrients to the coastal ocean, and surface concentrations of phosphate and silicate were 2- to 3-fold higher at our MRW stations than elsewhere (Fig. 2). Although surface concentrations of N+N were also elevated

at MRW stations, the increase in N availability was less than that of P, resulting in N:P ratios well below the Redfield Ratio as evidenced by the strongly negative  $N^*$  values in this habitat (Fig. 2D). As a result, surface waters of the MRW habitat were strongly nitrogen limited, a condition which will promote diazotrophy despite the presence of nutrients in surface waters. Under these conditions, the presence of high silica concentrations of up to 15  $\mu$ M near the river mouth will support diatom growth and provide a strong selective advantage to DDAs as long as the symbionts are able to supply the inorganic nitrogen required for growth.

The one host diatom sampled that was uniformly uninfected in MRW was Chaetoceros compressus, which showed single instances of infection by the epibiont Calothix rhizosoleniea in onshore (OnSW) and upwelling (UpW) waters, and sporadic infection in offshore waters (OSW). In all habitats, most of our C. compressus samples showed no infection by C. rhizosoleniea (Fig. 5G). This pattern suggests that the epibiotic association is relatively difficult to establish and does best under the less variable conditions offshore, where it is less likely to be disrupted physically. Interestingly, Gómez et al. (2005) found a low infection rate for C. compressus in the Sulu Sea and no infection in South China Sea, though they sampled only one station in the South China Sea. In contrast, the endosymbiotic associations involving Richelia intracellularis occurred in all habitats sampled, suggesting that it is more robust physically. These gross physical differences are also consistent with the contrasts in genome size reported by Hilton et al. (2013) and Caputo et al. (2018), which imply a tighter physical integration between the endosymbiotic R. intracellularis and its host than between epibiotic Calothrix rhizosoleniae and their host diatom, Chaetoceros compressus.

Infection intensity varied among diatom hosts, with the highest symbiont load occurring in *R. clevei* var. *communis* and *G. cylindrus*, and relatively low symbiont loads in *H. membranaceus* (Fig. 6). Prior studies have documented clear variations in the length, location, and number of *Richelia* and *Calothrix* trichomes associated their diatom partners, as well as the phylogenetic specificity of the symbionts in each symbiosis (Janson et al., 1999; Foster & Zehr 2006). The factors that promote multiple infection of DDA hosts are not fully understood, though our data clearly indicate that



at least some of the variation in infection rate is host-specific and likely reflects specific differences in the interaction between host and symbiont. The number of symbionts in a host cell will affect the carbon and nitrogen budgets of both partners in the symbiosis (Inomura et al., 2020), and the external nutrient environment can modulate the interaction between host and symbiont (Gao et al., 2022). While an increase in symbiont numbers will increase the total capacity for N<sub>2</sub>-fixation in the system, it will also reduce the host carbon subsidy available to support each symbiont's metabolic activity, including N<sub>2</sub>-fixation (Inomura et al., 2020). As a result, the number of cyanobacterial symbionts per host diatom reflects both external (N limitation) and internal (C limitation) factors.

Finally, all hosts showed a positive correlation between symbiont number and host size, reflecting the increased nitrogen demands of larger host cells (Fig. 7). This observation is consistent with the results of recent physiological models of N and C exchange between diatom hosts and diazotrophic symbionts (Inomura et al., 2020). Interestingly, the scaling of infection intensity with host size varied among the different hosts, with a greater increase in symbiont number with host size in smaller hosts (i.e., steeper least squares regression slope in Fig. 7). A Tukey test for significant differences among the slopes of these regressions (R version 4.2.1 with Ismeans and emmeans packages) revealed that only two pairwise contrasts are significant (G. cylindrus vs. R. clevei and R. clevei var. communis vs. R. clevei). Nonetheless, this overall pattern may reflect an inherent scaling of symbiont number with metabolically active host biomass (i.e., cytoplasm) since the host vacuole occupies a larger fraction of total internal volume as cell size increases (Strathmann 1967). We also note that we found much higher infection intensities (symbionts per host cell) in the SCS than were modeled by Inomura et al. (2020), so DDAs in our system may encompass physiological states and interactions beyond those that were simulated in their model.

## DDA niche partitioning

We have previously shown that our approach to defining phytoplankton habitats provides a robust tool for assessing differences in phytoplankton communities as a whole (Weber et al., 2019), and now

consider the distribution of DDA abundance and infection rate in different habitats of the SCS. The three most widely distributed DDAs showed broad overlap in distribution in the South China Sea. We were initially surprised to find intact DDAs in all water types, including the relatively fresh and nutrient rich Mekong River Waters (MRW, Fig. 6), but our nutrient data provide strong evidence for nitrogen limitation throughout our study region, including within the MRW habitat where the silica concentrations are consistently high. The broad distribution of DDAs implies that the associations are robust and that symbiosis plays an important role in supporting growth of the host diatoms in all habitats of the SCS. As noted above, all three of the most widely distributed DDAs we sampled showed relatively low abundances and infection rates in upwelling waters (Figs. 4, 5), suggesting that this was the least favorable habitat for DDAs of the waters we sampled. In our coastal upwelling water (UpW) nutrient concentrations, especially DIN, were higher than other habitats (see Weber et al., 2021) which may be a reason for the low infection rate of DDA hosts.

Our data also suggest at least some variation in DDA physiology among habitats. For example, we saw marked variation in cell size among DDA hosts, with individual diatoms differing in volume by orders of magnitude (Fig. 5). Interestingly, C. compressus host cells appear to fall into distinct size classes in the OnSW and OSW habitats, a pattern that also appears in R. clevei var. communis. Although these different host size classes may simply reflect normal growth and division in diverse populations, the relationship between host size and infection intensity suggests that these may also represent different strategies for hosting and interacting with symbionts. Specifically, large hosts with multiple symbionts and small hosts with one or two symbionts may reflect different optima for partitioning primary production between symbiotic partners. These physiological optima may be strongly driven by external factors such as light attenuation in the water column or depth of the mixed layer, both of which will be important in determining the total light energy available to the DDA. Further experimental and modeling studies may help resolve the nature of these interactions and strategies.



#### **Conclusions**

The South China Sea is a dynamic and hydrographically complex region where primary production is supported by riverine as well as oceanic nutrients. Although phosphate and silicate were both present in surface waters throughout our study area, the relatively low availability of inorganic nitrogen in solution provides an important competitive advantage to diazotrophic organisms and associations. DDAs were broadly distributed throughout our study region, with intact symbioses present in all of the habitats sampled, including waters directly affected by the MR outflow (MR habitat). DDA infection rates (frequency of hosts bearing symbionts) and infection intensities (number of symbionts per host) were lowest in the UpW habitat, where increased availability of nitrogen in surface waters may allow non-diazotrophs to compete effectively for other nutrients. DDA host diatoms varied widely in size and infection intensity in our study region, which may reflect different optimal strategies for allocating biomass and energy between host and symbiont.

Acknowledgements We thank the officers and crew of the R/V Falkor for their outstanding support of our work at sea, the Schmidt Ocean Institute for providing us with ship time, and the Institute of Oceanography in Nha Trang for providing shore-based logistical support for this project. The authors also want to acknowledge the reviewers and associate editor for constructive criticism for improvement of the manuscript. This work was partly supported by a grant of ship time from the Schmidt Ocean Institute. A grant from the National Foundation of Science and Technology of Viet Nam via project 106.06-2017.305 to L. N-N & H D-N and a grant from the German Science Foundation to M.V. (Vo487/13-1).

**Data availability** Data will be made available on reasonable request from the authors.

#### **Declarations**

**Conflict of interest** The authors declare that they have no known competing financial interests or personal relationships that could have appeared to influence the work reported in this paper.

# References

Bombar, D., P. H. Moisander, J. W. Dippner, R. A. Foster, M. Voss, B. Karfeld & J. P. Zehr, 2011. Distribution of diazotrophic microorganisms and nifH gene expression in the

- Mekong River plume during intermonsoon. Marine Ecology-Progress Series 424: 39–52.
- Capone, D. G., J. A. Burns, J. P. Montoya, A. Subramaniam, C. Mahaffey, T. Gunderson, A. F. Michaels & E. J. Carpenter, 2005. Nitrogen fixation by *Trichodesmium* spp.: An important source of new nitrogen to the tropical and subtropical North Atlantic Ocean. Global Biogeochemical Cycles 19: GB2024.
- Caputo, A., M. Stenegren, M. C. Pernice & R. A. Foster, 2018. A short comparison of two marine planktonic diazotrophic symbioses highlights an un-quantified disparity. Frontiers in Marine Science. https://doi.org/10.3389/fmars.2018.0000.
- Detoni, A. M. S., A. Subramaniam, S. T. Haley, S. T. Dyhrman & P. H. R. Calil, 2022. Cyanobacterial Diazotroph Distributions in the Western South Atlantic. Frontiers in Marine Science 9: 856643.
- Dippner, J. W., K. V. Nguyen, H. Hein, T. Ohde & N. Loick, 2007. Monsoon induced upwelling off the Vietnamese coast. Ocean Dynamics 57: 46–62.
- Dippner, J. W., N. N. Lam, D. N. Hai & A. Subramaniam, 2011. A model for the prediction of harmful algae blooms in the Vietnamese upwelling area. Harmful Algae 10: 606–611.
- Doan-Nhu, H., L. Nguyen-Ngoc, N. T. M. Anh, J. Larsen & N. C. Thoi, 2014. Diatom genus *Chaetoceros* Ehrenberg 1844 in Vietnamese waters. In Kociolek, J. P., M. S. Kulikovskiy, J. Witkowski & D. M. Kharvud (eds), Diatom Research Over Time and Space: Morphology, Taxonomy, Ecology and Distribution of Diatoms: From Fossil to Recent, Marine to Freshwater, Established Species and Genera to New Ones: Celebrating the Work and Impact of Nina Strelnikova on the Occasion of her 80th Birthday. J. Cramer in der Gebr. Borntraeger Verlagsbuchhandlung, Stuttgart.
- Follett, C. L., S. Dutkiewicz, D. M. Karl, K. Inomura & M. J. Follows, 2018. Seasonal resource conditions favor a summertime increase in North Pacific diatom-diazotroph associations. ISME J 12: 1543–1557.
- Foster, R. A. & J. P. Zehr, 2006. Characterization of diatomcyanobacteria symbioses on the basis of nifH, hetR and 16S rRNA sequences. Environmental Microbiology 8: 1913–1925.
- Foster, R. A., A. Subramaniam, C. Mahaffey, E. J. Carpenter, D. G. Capone & J. P. Zehr, 2007. Influence of the Amazon River Plume on distributions of free-living and symbiotic cyanobacteria in the western tropical north Atlantic Ocean. Limnology and Oceanography 52: 517–532.
- Foster, R. A., A. Subramaniam & J. P. Zehr, 2009. Distribution and activity of diazotrophs in the Eastern Equatorial Atlantic. Environmental Microbiology 11: 741–750.
- Foster, R. A., N. L. Goebel & J. P. Zehr, 2010. Isolation of Calothrix rhizosoleniae, Cyanobacteria. Strain Sc01 from Chaetoceros, Bacillariophyta. spp. diatoms of the subtropical North Pacific Ocean. Journal of Phycology 46: 1028–1037.
- Gao, M., G. Armin & K. Inomura, 2022. Low-ammonium environment increases the nutrient exchange between diatom-diazotroph association cells and facilitates photosynthesis and N2 fixation – a mechanistic modeling analysis. Cells 11: 2911.



- Goes, J. I., H. D. R. Gomes, A. M. Chekalyuk, E. J. Carpenter, J. P. Montoya, V. J. Coles, P. L. Yager, W. M. Berelson, D. G. Capone, R. A. Foster, D. K. Steinberg, A. Subramaniam & M. A. Hafez, 2014. Influence of the Amazon River discharge on the biogeography of phytoplankton communities in the western tropical north Atlantic. Progress in Oceanography 120: 29–40.
- Gomez, F., K. Furuya & S. Takeda, 2005. Distribution of the cyanobacterium *Richelia intracellularis* as an epiphyte of the diatom Chaetoceros compressus in the western Pacific Ocean. Journal of Plankton Research 27: 323–330.
- Grosse, J., D. Bombar, N. D. Hai, N. N. Lam & M. Voss, 2010. The Mekong River plume fuels nitrogen fixation and determines phytoplankton species distribution in the South China Sea during low- and high-discharge season. Limnology and Oceanography 55: 1668–1680.
- Gruber, N., 2019. A diagnosis for marine nitrogen fixation. Nature 566: 191–193.
- Gruber, N. & J. N. Galloway, 2008. An Earth-system perspective of the global nitrogen cycle. Nature 451: 293–296.
- Gruber, N. & J. L. Sarmiento, 1997. Global patterns of marine nitrogen fixation and denitrification. Global Biogeochemical Cycles 11: 235–266.
- Guiry, M., 2020. AlgaeBase http://www.algaebase.org
- Ha, D. T., S. Ouillon & G. V. Vinh, 2018. Water and suspended sediment budgets in the lower mekong from high-frequency measurements (2009–2016). Water 10: 846.
- Heinbokel, J. F., 1986. Occurrence of *Richelia intracellularis*, Cyanophyta. within the diatoms *Hemiaulus haukii* and *H. membranaceus* off Hawaii. Journal of Phycology 22: 399–403.
- Hilton, J. A., R. A. Foster, J. H. Tripp, B. J. Carter, J. P. Zehr & T. A. Villareal, 2013. Genomic deletions disrupt nitrogen metabolism pathways of a cyanobacterial diatom symbiont. Nature Communications 4: 1767.
- Hoang, Q. T., 1962. Phytoplankton in Nha Trang Bay 1: Diatoms: Bacillariales. Annales de la Faculté des Sciences de Saigon: 121–213
- Inomura, K., C. L. Follett, T. Masuda, M. Eichner, O. Prasil & C. Deutsch, 2020. Carbon transfer from the host diatom enables fast growth and high rate of N-2 fixation by symbiotic heterocystous cyanobacteria. Plants-Basel 9: 192.
- Janson, S., J. Wouters, B. Bergman & E. J. Carpenter, 1999. Host specificity in the Richelia-diatom symbiosis revealed by hetR gene sequence analysis. Environmental Microbiology 1: 431–438.
- Karsten, G., 1907. Das Indische Phytoplankton. Deutsche Tiefsee- Expedition 1898–1899. Bd. II 2 Teil. Wiss Ergeb Dsch Tiefsee-Exped "valdavia" 2: 138–221.
- Kimor, B., F. M. H. Reid & J. B. Jordan, 1978. An unusual occurrence of *Hemiaulus membranaceus* Cleve (Bacillariophyceae) with *Richelia intracellularis* Schmidt (Cyanophyceae) off the coast of Southern California in October 1976. Phycologia 17: 162–166.
- Lemmermann, E., 1899. Ergebnisse einer Reise nach dem Pacific., H. Schauinsland 1896/97. Abhandlungen Herausgegeben Vom Naturwissenschaftlichen Zu Bremen 16: 313–398.
- Lemmermann, E., 1905. Die Algenflora der Sandwich-Inseln. Ergebnisse einer Reise nach dem Pacific, H. Schauinsland

- 1896/97. Bot Jahrb Syst Pflanzengesch Pflanzengeogr 34: 607–663.
- Liu, Y., J. A. Bye, Y. You, X. Bao & D. Wu, 2010. The flushing and exchange of the South China Sea derived from salt and mass conservation. Deep Sea Research Part II 57: 1212–1220.
- Loick-Wilde, N., D. Bombar, H. Doan-Nhu, L. Nguyen-Ngoc, A. M. Nguyen-Thi, M. Voss & J. W. Dippner, 2017. Microplankton biomass and diversity in the Vietnamese upwelling area during SW monsoon under normal conditions and after an ENSO event. Progress in Oceanography 153: 1–15.
- Marconi, D., D. M. Sigman, K. L. Casciotti, E. C. Campbell, M. Alexandra Weigand, S. E. Fawcett, A. N. Knapp, P. A. Rafter, B. B. Ward & G. H. Haug, 2017. Tropical dominance of N2 fixation in the North Atlantic Ocean. Global Biogeochemical Cycles 31: 1608–1623.
- Mulholland, M. R., P. W. Bernhardt, B. N. Widner, C. R. Selden, P. D. Chappell, S. Clayton, A. Mannino & K. Hyde, 2019. High rates of N2 fixation in temperate, western North Atlantic coastal waters expand the realm of marine diazotrophy. Global Biogeochemical Cycles 33(7): 826–840.
- Nguyen, T. A., 1997. Primary production and ecological effects of upwelling in the Southern Central Viet Nam. In Vo, V. L. (ed), Contributions on Coastal Strong Upwelling in Southern Central Viet Nam. Science and Technique Publishing House, Hanoi.
- Okamura, K., 1907. Some *Chaetoceros* and Peragallia of Japan. Shokubutsugaku Zasshi 21: 89–106.
- Paerl, R. W., R. A. Foster, B. D. Jenkins, J. P. Montoya & J. P. Zehr, 2008. Phylogenetic diversity of cyanobacterial narB genes from various marine habitats. Environmental Microbiology 10: 3377–3387.
- Pham, H. H., 1969. Marine Algae of South Viet Nam, Trung-Tâm Học-Liệu Press, Saigon:
- Round, F. E., R. M. Crawford & D. G. Mann, 1990. The Diatoms: Biology & Morphology of the Genera, Cambridge University Press, Cambridge:
- Schvarcz, C. R., S. T. Wilson, M. Caffin, R. Stancheva, Q. Li, K. A. Turk-Kubo, A. E. White, D. M. Karl, J. P. Zehr & G. F. Steward, 2022. Overlooked and widespread pennate diatomdiazotroph symbioses in the sea. Nature Communications 13: 1–9.
- Shaw, P. T. & S. Y. Chao, 1994. Surface circulation in the South China Sea. Deep Sea Research Part I 41: 1663–1683.
- Sherman, D. M., D. Tucker & L. A. Sherman, 2000. Heterocyst development and localization of cyanophycin in N2-fixing cultures of *Anabaena* sp. PCC 7120 (Cyanobacteria). Journal of Phycology 36: 932–941.
- Sournia, A., 1970. Les cyanophycees dans le plancton marin. Année Biologique 9: 63–76.
- Strathmann, R. R., 1967. Estimating the organic carbon content of phytoplankton from cell volume or plasma volume. Limnology and Oceanography 12: 411–418.
- Subramaniam, A., P. L. Yager, E. J. Carpenter, C. Mahaffey, K. Bjorkman, S. Cooley, A. B. Kustka, J. P. Montoya, S. A. Sanudo-Wilhelmy, R. Shipe & D. G. Capone, 2008. Amazon River enhances diazotrophy and carbon sequestration in the tropical North Atlantic Ocean. Proceedings of the National Academy of Sciences 105: 10460–10465.



- Sundstrom, B. G., 1984. Observations on *Rhizosolenia clevei* Ostenfeld, Bacillariophyceae. and *Richelia intracellularis* Schmidt. Botanica Marina 27: 345–355.
- Tomas, C. R. & G. R. Hasle, 1997. Identifying Marine Phytoplankton, Academic Press, San Diego:
- Venrick, E. L., 1974. The distribution and significance of *Richelia intracellularis* Schmidt in the North Pacific Central Gyre. Limnology and Oceanography 19: 437–445.
- Villareal, T. A., 1989. Division cycles in the nitrogen-fixing Rhizosolenia (Bacillariophyceae)-Richelia (Nostocaceae) symbiosis. British Phycological Journal 24: 357–365.
- Villareal, T. A., L. Adornato, C. Wilson & C. A. Schoenbaechler, 2011. Summer blooms of diatom-diazotroph assemblages and surface chlorophyll in the North Pacific gyre: a disconnect. Journal of Geophysical Research. https://doi. org/10.1029/2010JC006268.
- Voss, M., D. Bombar, N. Loick & J. W. Dippner, 2006. Riverine influence on nitrogen fixation in the upwelling region off Vietnam, South China Sea. Journal of Geophysical Research. https://doi.org/10.1029/2005GL025569.
- Voss, M., D. Bombar, J. W. Dippner, D. N. Hai, N. N. Lam & N. Loick-Wilde, 2014. The Mekong River and its influence on the nutrient chemistry and matter cycling in the Vietnamese coastal zone. In Bianchi, T. S., M. A. Allison & W. J. Cai (eds), Biogeochemical Dynamics at Major Rivercoastal Interfaces: Linkages with Global Change. Cambridge University Press, New York.
- Ward, B. A., S. Dutkiewicz, C. M. Moore & M. J. Follows, 2013. Iron, phosphorus, and nitrogen supply ratios define the biogeography of nitrogen fixation. Limnology and Oceanography 58: 2059–2075.
- Weber, S. C., E. J. Carpenter, V. J. Coles, P. L. Yager, J. Goes & J. P. Montoya, 2017. Amazon River influence on nitrogen fixation and export production in the western tropical North Atlantic. Limnology and Oceanography 62: 618–631.

- Weber, S. C., A. Subramaniam, J. P. Montoya, D. N. Hai, N. N. Lam, J. W. Dippner & M. Voss, 2019. Habitat delineation in highly variable marine environments. Frontiers in Marine Science 6: UNSP112.
- Weber, S. C., N. Loick-Wilde, J. P. Montoya, M. Bach, H. Doan-Nhu, A. Subramaniam, I. Liskow, L. Nguyen-Ngoc, D. Wodarg & M. Voss, 2021. Environmental regulation of the nitrogen supply, mean trophic position, and trophic enrichment of mesozooplankton in the Mekong River plume and southern South China Sea. Journal of Geophysical Research: Oceans 126(8): e2020JC017110.
- Wu, J., S.-W. Chung, L.-S. Wen, K.-K. Liu, Y.-L. Lee Chen, H.-Y. Chen & D. M. Karl, 2003. Dissolved inorganic phosphorus, dissolved iron, and *Trichodesmium* in the oligotrophic South China Sea. Global Biochemical Cycles 17: 1008. https://doi.org/10.1029/2002GB001924.
- Wyrtki, K., 1961. Physical Oceanography of the Southeast Asian Waters, Vol. 2. University of California, Scripps Institution of Oceanography, La Jolla:
- Zehr, J. P. & D. G. Capone, 2020. Changing perspectives in marine nitrogen fixation. Science. https://doi.org/10.1126/ science.aay9514.

**Publisher's Note** Springer Nature remains neutral with regard to jurisdictional claims in published maps and institutional affiliations.

Springer Nature or its licensor (e.g. a society or other partner) holds exclusive rights to this article under a publishing agreement with the author(s) or other rightsholder(s); author self-archiving of the accepted manuscript version of this article is solely governed by the terms of such publishing agreement and applicable law.

